Fermi National Accelerator Laboratory

FERMILAB-Pub-90/18

Muon Rates at the SSC*

Dan Green
Fermi National Accelerator Laboratory
P.O. Box 500
Batavia, Illinois 60510

and

David Hedin
Northern Illinois University
DeKalb, Illinois 60115

January 1990

* To be submitted to Nucl. Instrum. Methods A.

Operated by Universities Research Association Inc. under contract with the United States Department of Energy

MUON RATES AT THE SSC

Dan Green
Fermilab, Batavia IL 60510
David Hedin
Northern Illinois University, DeKalb IL 60115

This paper presents calculations of muon rates at the SSC. It will give muon distributions in angle and p_T for a range of detector thicknesses and will separately give the rates from various sources. In particular, we will attempt to make a crisp definition of the absorber thickness which is needed for good muon detection in SSC detector enviroments. This paper is a continuation of previous studies.[1]

There are five sources of particles which produce hits in a SSC muon detector:

1. $\pi^{\pm}, K^{\pm}$ and K_L decays;
2. prompt muons (c, b, t and W decays);
3. hadron punchthrough;
4. cosmic rays;
5. low energy particle backgrounds.

We will discuss items 1-3. The rates from 1 and 2 are straightforward to estimate. The π and K decay rates depend on the path length to their first interaction point, while those muons from heavier particle decays (prompt) depend only upon the production mechanism. What are not particularly well understood are the backgrounds due to punchthroughs, by which we mean the existence of particles deep in hadronic showers which escape into the muon detection system. As we will see later, these particles can be either hadrons or muons. For thick absorbers they are most likely to be muons. Punchthroughs can be reduced relative to other muon sources by adding absorber. Thus an important question in designing SSC muon detectors is the necessary thickness.

We will first discuss the rate and kinematic distributions of particles produced by hadronic interactions. From this, we will develop a model for punchthroughs and use two techniques (one semi-analytical and one using ISAJET) to integrate over the particle distributions in pp interactions at 40 TeV. This will give us the rate and kinematic distributions of particles in an SSC muon detector and allow us to estimate the absorber thickness needed for muon identification and triggering.

I. Hadronic Interactions in Thick Absorbers

In order to begin to understand the punchthrough phenomenon it is important to first gather up existing data and try to understand the general characteristics that emerge. In Fig. 1 is shown data from Lab E neutrino experiments[2] taken during test runs with incident hadrons. The probability of finding a muon at a momentum fraction z of the hadron is given, where the incident hadronic energy varies from 50 to 200 GeV. The "fragmentation function", D(z), is defined such that the muon momentum is referred to the front of the absorber. The total absorber thickness[3] in this data is 26 λ_0 and the mean density of the detector is 4.2 gm/cm^3. The first thing that strikes you is that there is an approximate scaling law. The fragmentation function is roughly independent of the incident hadron momentum, at least within the accuracy of the data.

Other data[4] from experiment E-379 are shown in Fig. 2 for incident hadron energies of 40, 75, 150, and 225 GeV. Again there seems to be a scaling behavior. It's also clear that the two data sets shown in Figs. 1 and 2 agree. For E-379 the total absorber depth was 18.5 λ_0 and the mean density was 6.1 gm/cm^3. Later we will see that we expect D(z) to be proportional to the density. These two data sets are not of sufficient accuracy to support this prediction.

First let us see if we can understand this scaling behavior with the most simple minded model that we can make. Assume that a hadron of momentum p is incident on an absorber. It begins to shower at a depth of one λ_0. That shower creates a mean multiplicity of hadrons, $< n >$, with momentum k. Those hadrons (pions) must decay into muons of momentum q before the next shower, that is within one more λ_0. We will ignore the difference between k and q. The relationship between the lab momentum of a secondary, a primary, and the Feynman scaling variable x is approximately, k = xp. In this simple minded model the muons from the decay of first generation pions constitute punchthrough. If one goes deeper in the absorber, one simply ranges out muons of higher momentum. Obviously, this picture ignores multi-generations, and so it will do a poor job on pile up at low momentum. Fluctuations in the showers are also totally ignored.

The assumptions in this model for production are given below in Eq. 1. An additional assumption is that there is a rapidity plateau. The production cross section is constant in y up to the kinematically allowed maximum value y_{max}.

$$\begin{aligned} d\sigma/dy &= a \\ y_{max} &= ln(\sqrt{s}/m) \\ x &\approx (m_T/\sqrt{s})e^y \quad . \end{aligned} \tag{1}$$

Obviously the mean multiplicity is proportional to the width of the rapidity plateau. The differential cross section as a function of Feynman x is:

$$\begin{aligned} < n > &= 2ay_{max} \\ dx/dy &\approx x \\ d\sigma/dx &\approx [< n > /2y_{max}](1/x) \quad . \end{aligned} \tag{2}$$

Clearly the idea is to relate the observed scaling behavior of the punchthrough fragmentation function to the well known scaling behavior of secondary production processes in hadron collisions. "Jets" are also known to fragment with a scaling behavior.[5]

As mentioned before, Feynman x is approximately the laboratory momentum fraction carried off by the secondary, which is defined to be z. The secondary decay probability is approximately proportional to one over the laboratory momentum and therefore:

$$\begin{aligned} x &\approx k/p = z \\ P_D &\approx (\lambda/c\tau)(m/k) \\ D_\mu(z) &\approx [< n > /2y_{max}](\lambda/c\tau)(m/p)(1/z^2) \quad . \end{aligned} \tag{3}$$

This simple expression for the fragmentation function depends on the density of the material, and has a rough scaling shape. However, it is explicitly dependent on the momentum of the incident hadron. Since the data in Figs. 1 and 2 only span a factor of five in momentum, we will pick (for a numerical comparison) 25 GeV incident momentum. This simple expression for the fragmentation function is shown in Fig. 3.

Surprisingly enough, both the shape and the magnitude roughly agree with the data shown in Figs. 1 and 2. If anything the data falls more rapidly, which appears to be a reflection of the fact that the rapidity plateau does not extend to the kinematic limit. Typically this behavior is parameterized in the form of a power law in (1-x). Hence, we also show in Fig. 3 the simple fragmentation function multiplied by $(1\text{-}z)^4$. This modified form is in much better agreement with the data at high values of x or z, i.e. values around 0.5.

Another comparison of interest is to look at the relationship between this data, which is for muons escaping from thick absorbers with incident hadrons, and data which only ask for something to punchthrough into a detector element downstream of an absorber. If we parameterize the data of Figs. 1 and 2 using a fragmentation function which is the sum of two exponentials, then this form is easily integrated to get the muon punchthrough probability as shown below:

$$\begin{aligned} D_\mu(z) &\approx a_1 e^{-b_1 z} + a_2 e^{-b_2 z} \\ P_\mu(\lambda, p) &\approx (a_1/b_1) e^{-b_1 k_{min}/p} + (a_2/b_2) e^{-b_2 k_{min}/p} \\ k_{min} &\approx (dE/dx) L, L = \text{absorber length} \quad . \end{aligned} \tag{4}$$

Shown in Fig. 4 is the probability for a pion to decay in a two meter decay length as a function of momentum. In comparison, the probability for the pion to punchthrough in an absorber of total thickness 14 λ_0 is also shown. First note that punchthroughs, in this situation, dominate over decays for momenta > 20 GeV. Next note that the punchthrough probability is effectively one for momenta above about 600 GeV. This means that, if one only measures the appearance of some particle exterior to a 14 λ_0 thick absorber, one essentially has no rejection power against hadrons above 600 GeV. At rapidity y = 3 this means hadrons with transverse momenta > 60 GeV.

The hadron punchthrough points are a fit[6] to the WA1 data:

$$\begin{aligned} P(\lambda, p) &\approx exp[(\lambda - \lambda')/\lambda_{eff}] \\ \lambda' &= 1.53 p(GeV)^{0.33} \lambda_0 \\ \lambda_{eff} &= 0.89 p(GeV)^{0.165} \lambda_0 \quad . \end{aligned} \tag{5}$$

The punchthrough probability is one for depths $< \lambda'$. Beyond a depth of λ', the punchthrough probability falls off exponentially with an effective absorption length which is greater than λ_0. What's extremely interesting is that the integrated muon fragmentation function agrees well with our parameterization of the WA1 hadronic punchthrough data in the region of validity, which means for momenta between about 20 and 100 GeV. Note

that a depth of 14 λ_0 of iron ranges out decay muons from pion secondaries up to about 2.8 GeV. This means that for 100 GeV incident momentum, the minimum value for z is roughly 0.028. There are no data for $z < 0.03$ in Figs. 1 and 2. Low z means multi-generation pileup, so we expect that the comparison between the integrated muon fragmentation function, Eq. 4, and the WA1 fit, Eq. 5, may not be valid there.

The success of this comparison (within factors of three) leads us to believe that deep punchthrough consists largely of low energy muons from the decay of shower products rather than unquenched hadron showers themselves. This is certainly true at large depths where the hadron showers are quenched - i.e., the mean number of shower particles falls below one. To set the scale, at 14 λ_0 depth, the mean number of hadronic shower particles is less than 1 for incident hadron momenta less than 1 TeV. Thus, at this depth, and for hadrons below 1 TeV, the punchthrough consists mostly of muons.[7]

If punchthrough consists of muons, and we are trying to detect muons, what more can we do to get rid of them aside from measuring their momentum and/or ranging them out. Obviously, one thing is to track the incident particle and the outgoing muon and see if the exit position and angle are consistent with pure Coulomb scattering of an incident muon. For example, for 14 λ_0 in steel, multiple scattering causes a projected transverse momentum impulse of 163 MeV. This means that a 100 GeV muon has a one standard deviation angular matching error of 1.6 mrad. By comparison, the secondary pions in the shower have a mean transverse momentum of about 333 MeV:

$$\begin{aligned} &< \kappa_T > = 2/\alpha = 0.33\ GeV \\ &d\sigma/dyd\kappa_T^2 \approx [< n > \alpha^2/4y_{max}]e^{-\alpha\kappa_T} \quad . \end{aligned} \tag{6}$$

Given the production characteristics for low transverse momentum inclusive pion production, it is easy to work through the joint fragmentation function for momentum fraction z and angle θ shown below:

$$\begin{aligned} &\theta \approx \kappa_T/k \approx \kappa_T/zp \\ &D_\mu(z,\theta) \approx [< n > (\alpha p)^2/2\ y_{max}](\lambda/c\tau)[\theta e^{-\alpha z\theta p}] \quad . \end{aligned} \tag{7}$$

As an immediate check, if one takes the expression given in Eq. 7 and integrates over all angles one recovers the muon fragmentation function given in Eq. 3. Conversely, if the momentum fraction is integrated over, the fragmentation function as a function of angle is:

$$\begin{aligned} &D_\mu(\theta) \approx [< n > (\alpha m)/2y_{max}](\lambda/c\tau)e^{-\alpha\theta k_{min}} \\ &< \theta_\mu > \approx 1/k_{min}\alpha \quad . \end{aligned} \tag{8}$$

Note that so far we find that the mean angle for muon punchthrough depends on the minimum value of the momentum of the muons due to the depth of the material. Otherwise, the angular fragmentation function is a scaling object, which is independent of

the momentum of the incident hadron. For example, at a 14 λ_0 depth in steel, the mean angle is 74 mrad for the space angle or 50 mrad for the projected angle.

Test beam data[8] taken for D0 are shown in Fig. 5. What is plotted is the Lorentzian half width, $\Gamma/2$, of the punchthrough for hadron showers at depths of 7.3 and 14.6 λ_0 for hadron momentum of 100 and 150 GeV. The first thing to note is that the width is rather independent of momentum, as one expects from our previous estimate, Eq. 8. The production radius, using Eq. 8, is roughly $R_{prod} \approx [\alpha(dE/dx)]^{-1}$, which is a constant independent of momentum and depth. This prediction is shown in Fig. 5 as the dashed line. Obviously, it is not a good representationof the data. We must improve the model.

So far we have ignored the multiple scattering of the soft decay muons as they pass through the absorber. Assuming that the exit size is due to scattering, and that it is dominated by particles with z near z_{min} (given the $1/z^2$ distribution), then:

$$\begin{aligned} \beta &\equiv 0.021\ GeV \\ R_{ms} &\equiv [\beta/(dE/dx)]\sqrt{L/x_o} \quad . \end{aligned} \tag{9}$$

This dependence on depth is also shown in Fig. 5. It appears to be qualitatively correct, in that it is independent of incident momentum and weakly ($\sqrt{L}$) dependent on depth of absorber. The magnitude is also in rough agreement. More detailed data from Lab E will soon be available. This data[9] indicates a weak dependence of R on L ($\approx \sqrt{L}$), and a rather weak dependence of R on p, as expected in our very crude model.

Clearly, one can use the difference in width of the spatial distributions of isolated muons incident on the absorber and of the punchthrough muons from incident hadrons to get another rejection factor. One asks; is this the parent or is it a momentum reduced multiply scattered secondary decay muon?

Data taken to study the D0 muon system are shown in Fig. 6. The curves are punchthrough probabilities for hadrons as a function of hadron momentum at a depth of 7.3 λ_0 and 14.6 λ_0. In addition, the probability of data also surviving a two dimensional Coulomb cut is shown. This cut leaves a residual punchthrough probability after making a 2σ cut in the exit position of the track, requiring the punchthrough track to be within that cone. Clearly, there is a substantial rejection to be had. The rejection factor also increases with momentum, since the punchthrough radius is roughly momentum independent (as we saw in Fig. 5), while the Coulomb cone has a radius that decreases with momentum.

Also indicated in Fig. 6 is the result of a rough calculation using a two standard deviation multiple scattering error, and defining the rejection factor to be the square of the 2σ multiple scattering width, divided by $< \theta_\mu > /\sqrt{2}$. That rejection factor, as plotted in Fig. 6, is reasonably close to what is observed in the data.

$$\begin{aligned} REJECTION &\equiv [2\theta_{ms}/(< \theta_\mu > /\sqrt{2})]^2 \\ \theta_{ms} &= (\beta\sqrt{L/x_o})/p \quad . \end{aligned} \tag{10}$$

Clearly, if the momentum of an incident track is known, then a "Coulomb cone" can be defined for the exit position with respect to the incident position. The resulting cut

improves with momentum, thus tending to cancel the rise of the punchthrough probability with momentum (see Fig. 6).

II. Rates in SSC Muon Detectors

The studies of existing test beam data presented above allow us to make a parameterization of the spectrum of exit momentum and angle for a hadron incident on a block of absorber. This means that we can quantitatively compare various sources of prompt muons and select an absorber thickness in a decisive way. The selection criterion chosen here is that punchthrough muons should be reduced below decay muons and below the signal due to prompt muons from some interesting physical process.

In principle, with isolated muons the task is rather straightforward, but it seems unlikely that one should restrict oneself to that sort of environment for a benchmark process. What is appealing about muons is that one can identify them in hostile environments such as in the core of jets. In fact, for jet flavor tagging it is necessary to work in that enviroment. Therefore, it is incumbent on the designer of a muon system to retain that advantage and be able to tag and identify muons in the core of jets.

We have chosen to do this calculation in two ways. We will first use a semi-analytical model. This will allow us to qualitatively understand how the produced jets fragment into hadrons, which then give muons. We will then repeat this using an ISAJET-based model. This will have better integration over items such as fragmentation and structure functions. The two techniques yield similar results for the relative contributions of different sources. The ISAJET calculation gives more precise values for the rate at different angles and p_T.

The jet cross section at the SSC (at least at 90^o) has a momentum spectrum that goes like $1/p^3$, which is due to the elementary 2-to-2 Rutherford scattering process.[10] Heavy flavors, in lowest order, arise from gluon-gluon fusion. Prompt muons arise from heavy flavor production followed by three body semileptonic decay, with branching ratios of order 1/9 (which follows from simple quark counting).

Shown in Fig. 7 are the differential cross sections $(d\sigma/dydp_T)_{y=0}$ for jets, heavy flavors, and prompt muons from semileptonic decays. Clearly, a physics driven criterion is to design a muon system in which the prompt muons from heavy flavors can be tagged cleanly with respect to all other background sources. The cross section scale is also important.[11] If the SSC runs at its design luminosity of $10^{33}\mathrm{cm}^{-2}\mathrm{sec}^{-1}$, then in a one year run at 1/3 efficiency (10^7 live seconds), there will be one muon at a p_T of 1 TeV per unit of rapidity per GeV. Thus, it seems unlikely that one needs to worry about large samples of muons with transverse momenta > 1 TeV.

What about hadronic backgrounds? First one needs to let the jets fragment into pions. The differential cross section estimate for that is shown in Fig. 8. Having fragmented the pions, one can get a decay background estimate for a two meter decay length. That background is also shown in Fig. 8. In making this estimate, the parent jet spectrum was assumed to be Rutherford like. The fragmentation function for jets fragmenting into pions was taken from UA1 data.[5] That data was approximately fit to an exponential fragmentation function:

$$d\sigma/dp \approx 1/p^3$$
$$D(z) = ae^{-bz}, a_\pi \approx 20, b_\pi \approx 8.6 \quad . \tag{11}$$

One of the nice properties of an exponential fragmentation function is that such a soft fragmentation, convoluted with a power law production spectrum, leads to the same power law spectrum for the fragment with a reduced cross section:[10]

$$d\sigma/dk = \int_k^\infty [d\sigma/dp] D(z) dp/p$$
$$(d\sigma/dk)/(d\sigma/dp) \approx 2a_\pi/b_\pi^3 \quad . \tag{12}$$

with k being the momentum of the fragment, in this case the exiting muon as opposed to p the momentum of the particle incident on the absorber.

Comparing Fig. 7 and Fig. 8, one can see that decays dominate over the signal for transverse momenta below 10 GeV. This statement assumes that the central tracking has no kink rejection factor, i.e. no additional rejection against decays. Above k_T of 10 GeV, the muons from heavy flavors in jets dominate over decays and do so by at least a factor of 10 for $k_T > 350$ GeV. This means that decay muons are under control as a source of background if we look at reasonably high mass dijet events.

What about punchthrough backgrounds? In principle, this is the dominant background. For a depth of 14 λ_0 we know the punchthrough exceeds the decay background (Fig. 4) for transverse momenta greater than 20 GeV. Using the integrated muon fragmentation function (Eq. 4) and the pion spectrum (Fig. 8), we find the rejection fraction for any hit beyond a depth of 14 λ_0. That rate is shown in Fig. 9.

The total punchthrough rate exceeds the prompt rate for transverse momenta > 30 GeV. Then for all p_T, a combination of decay and punchthrough background exceeds the prompt rate of muons. This is clearly unacceptable. We assume that, for flavor tagging, you are in the core of a jet and thus cannot depend on a central tracker to give you the momentum. In any case, the momentum must be measured after the absorber.

In many systems such as D0,[12] the last few absorption lengths of material exterior to the precision calorimetry are in the form of magnetized iron and are used to make a modest momentum measurement so as to reduce punchthrough. In this case, instead of using the integral punchthrough probability (Eq. 4), we use the differential probability (Figs. 1, 2) folded into the pion spectrum (Eq. 12). The rejection factor, for a fragmentation function consistent with the data shown in Figs. 1 and 2, is $\approx 4 \times 10^{-5}$. This reduction assumes that you have indeed measured the momentum. What accuracy does one need? Also shown in Fig. 9 is the result of smearing the muon momentum by $\pm 20\%$ which is appropriate to 1 m (≈ 6 λ_0) of magnetized steel exterior to 8 λ_0 of precision calorimetry. The steeply falling input spectrum means that a very crude measurement is quite dangerous. For $k_T > 300$ GeV, the momentum measured punchthrough with a 20% momentum measurement still exceeds the prompt rate. A crude measurement also comprimises the triggering scheme since it allows leakage from the enormously higher rates at low k_T.

Moreover, one may also use the vertex position of the event, and the tracking before and after the magnetized iron (which comes for free with the momentum measurement) in order to impose a two dimensional Coulomb cut. We have already discussed the rejection factor for those cuts. Note that one need not depend on finding the associated track in the core of a jet using central tracking. It is important to have stand alone muon capability up to

a luminosity of $10^{34}\text{cm}^{-2}\text{sec}^{-1}$ since the SSC luminosity is only limited to $10^{33}\text{cm}^{-2}\text{sec}^{-1}$ by synchrotron radiation. Hence, upgrades in luminosity are likely, and a dependence only on central tracking appears to be a bad bet.

Using the rejection factors which we roughly calculated using the simple model (or using the D0 test data shown in Fig. 6), we can estimate a maximum reduction in the momentum measured punchthrough rate by imposing these Coulomb cuts.[13] The resulting spectrum is shown in Fig. 9. This estimate implies one can always reduce the punchthrough rate (above about 20 GeV) to be well below the prompt rate. This is the criterion which we set out to achieve, to be able to cleanly measure muons from heavy flavors in a jet environment.

We have also used the ISAJET program (version 5.20) to generate proton-proton interactions at 40 TeV and then determine the rates from items 1-3. For this calculation, we used two-jet and W events with p_T from 5 to 10,000 GeV/c. Those pions and kaons which decay before interacting in the calorimeter and whose decay muons have enough energy to penetrate the absorber are defined as decays. The decay rate is directly proportional to the size of the central tracking region. We assume a cylinder with a 2.5 m radius and 10 m total length. This is the size of the largest central region we have seen considered.[14]

Prompt muon rates from heavy quark decays and W decays are also straightforward to estimate. Top and W decays can be differentiated from b or c decays (and from other muon sources) by their isolation. As such, they are usually a more important source of background to other heavy particle decay to muons (such as Z's). We have assumed a top mass of 120 GeV. The rate versus absorber thickness for both decay and prompt muons is only a function of energy loss in the absorber.

In determining the punchthrough rate, four different detection scenarios are possible:

a. Measure momentum only in inner region, no exiting measurement;
b. Measure momentum only in inner region, measurement of exiting position and angle;
c. Measure momentum exiting absorber;
d. Measure momentum before and after absorber.

Figure 10 shows the k_T distribution for punchthoughs after 14 λ_0 in the region $|\eta| < 1$ assuming a), b) and c). Those in a) assign each hadron the WA1 weight and use the hadron's p_T as the muon's k_T. Item b) multiplies the weighting factor using the Coulomb cut discussed above but still assigns the hadron p_T to the muon. For this Figure, we used a factor of $125/p^2$ up to 200 GeV (and assume that above 200 GeV the reduction factor is the 200 GeV value). The curve for c) uses the WA1 weight with the D(z) distribution in Figs. 1 and 2. As discussed above, an outer measurement of the muon momentum even with resolution of order 20% will dramatically decrease the rate at large k_T. Given a momentum measurement both before and after the absorber (which is feasible in the central region of a solenoidal detector), it should be possible to reduce the punchthrough rate even further.

The angular rates for particles exiting 14, 24, and 40 λ_0 of iron are given in Figure 11 (with the two hemispheres being summed). The same thickness is assumed at every angle. Table 1 summarizes the rates for thicknesses from 9-45 λ_0 and for various pseudorapidity intervals.

Table 1: Muon Rates* versus Absorber Thickness

Thickness		$0 < \|\eta\| < 3$	$0 < \|\eta\| < 1$	$1 < \|\eta\| < 2$	$2 < \|\eta\| < 3$
	All	28,000	400	4100	23,000
$9\lambda_0$	punch	4,900	70	420	4,400
	prompt	400	16	130	250
	All	18,000	250	2700	15,000
$12\lambda_0$	punch	430	5	30	400
	prompt	400	16	130	250
	All	11,000	130	1500	9600
$15\lambda_0$	punch	40	0.4	3	40
	prompt	380	13	120	250
	All	6800	80	700	6000
$18\lambda_0$	punch	5	-	0.4	5
	prompt	270	13	70	190
	All	4400	50	460	3900
$21\lambda_0$	punch	0.7	-	-	0.7
	prompt	270	10	70	190
	All	2700	30	270	2400
$25\lambda_0$	punch	-	-	-	-
	prompt	270	10	70	190
	All	900	12	70	800
$35\lambda_0$	punch	-	-	-	-
	prompt	150	7	10	135
	All	400	2	24	340
$45\lambda_0$	punch	-	-	-	-
	prompt	140	0.6	7	130

* rates in μb summed over p_T

Figure 12 gives the k_T distribution for an absorber thickness of 14 λ_0 assuming punchthroughs are measured using technique c). Decays dominate the rate and are predominantly at low-k_T. The total rate is 13 mb with 30 μb having k_T greater than 5 GeV/c. Figure 13 gives the relative fraction of exiting particles from prompt, decay and background sources. Above about 15 GeV/c, prompt sources (heavy quarks) begin to dominate with the rate from either π/K decays or punchthroughs falling to about 10^{-3} above a few hundred GeV.

The conclusion from the above rate estimates is that one must measure the momentum exterior to the absorber, but that this measurement need not be particularly accurate. The total absorber need not be excessively thick. Depths for calorimetry and magnetized steel comparable to those which are used in the D0 detector should be adequate. D0 was optimized for electroweak energy scales, which are at least an order of magnitude below those which are of interest in SSC detectors. If one does not measure the momentum

exterior to the main absorber, then one is restricted to physics in which one studies isolated muons. Even in the case of isolated muons, the redundant (though crude) exterior measurement protects you against mismeasures in the central tracker, which notoriously tend to promote lower momentum tracks to high momentum tracks. It is cheaper to measure punchthrough than to range it out, as a glance at Eq. 4 tells you. The optimal procedure is perhaps to have a fairly thin absorber (14 λ_0). After removing the 8 to 10 λ_0 needed for precision calorimetric measurements, that leaves of order 6 λ_0 which is sufficient to make a modest momentum measurement using magnetized iron as the absorber. That measurement buys you between four and five orders of magnitude in punchthrough rate. Simply stated it appears to be cheaper to get that factor from the momentum measurement than from adding tens of thousands of tons of steel.[1]

1. D. Carlsmith, et. al, "SSC Muon Detector Group Report," Proc. of the 1986 Summer Study on the Physics of the Superconducting Supercollider, Snowmass, 405 (1986).
2. B. Schemm, Ph.D. Thesis, University of Chicago, August (1988).
3. Unless stated otherwise, we assume throughout this note that 1 λ_0 of absorber is 16.8 cm of iron and gives an energy loss of 195 MeV to minimum ionizing particles.
4. K. Lang, Ph.D. Thesis, University of Rochester (1985).
5. V. Barger and R.J Phillips, "Collider Physics", Addison-Wesley (1987).
6. D. Green, "Muon Triggering at Small Angles", Proc. of the Workshop on Triggering, Data Acquisition and Computing in Hadron-Hadron Colliders, Fermilab (1985).
7. Monte Carlo calculations using GEANT confirm this as well as reproducing the measured fragmentation function of particles exiting a thick absorber. Roger McNeil, private communication.
8. D. Green, et. al, NIM **A244**, 356 (1986).
9. H. Schellman and P. Sandler, private communication; paper submitted to Phys. Rev. D.
10. D. Green, Fermilab CONF-89/70.
11. R.K. Ellis and J. Rohlf, "Summary Report of the Jet Study Group", Proc. of the 1984 Summer Study on the Design and Utilization of the Superconducting Super Collider, Snowmass, 203 (1984).
12. D0 Design Report, Fermilab (1984).
13. This estimate assumes that there is no correlation between the Coulomb cut and the fragmentation function. Though there are some cases where this is wrong (e.g a non-interacting hadron), we feel that it is a good first approximation.
14. For example, the Large Solenoid Detector. "Report of the Collider Group", submitted to the Proc. of the Workshop of Physics at Fermilab in the 1990's, Breckenridge (1989).

FIGURE CAPTIONS

1. Data from Lab E on D(z) for • 50, ■ 100 and ▼ 200 GeV incident hadron energy.

2. Data from E-379 on D(z) for o 40, □ 75, ▽ 150 and △ 225 GeV incident hadron energy.

3. Simplistic D(z) model for ⊙ rapidity plateau and • $(1\text{-}z)^4$ at 25 GeV incident energy.

4. Probability for detection at a depth of 14 λ_0 due to • decay in R = 2 m, and o punchthrough. Also shown is the integral of a curve, ⊙, which fits the data of Figs. 1 and 2.

5. D0 test data on shower widths for 100 and 150 GeV incident hadron energy at depths of 7.3 and 14.6 λ_0. The dashed curve is the simplistic shower width due to production, while the solid curve is the shower width due to multiple scattering.

6. D0 test beam data for punchthrough probability and for reduction due to a "Coulomb cut." A simplistic model estimate, ⊙, is also shown.

7. **Differential cross section estimates for jets, heavy flavors, and prompt muons from heavy flavor decay at $\sqrt{s} = 40$ TeV.**

8. **Differential cross section estimates for jets, π from jet fragmentation, and μ from pion decay in a R = 2 m space.**

9. Differential cross sections for π punchthrough at a 14 λ_0 depth, o, if momentum is measured, •, and if a "Coulomb cut," ⊙, is imposed.

10. Punchthrough rate in cm^2/GeV versus k_T assuming (a) the hadron is only measured in the inner tracking; (b) the hadron's momentum is measured in the inner tracking but a trajectory is measured after the absorber; and (c) the momentum is measured after the absorber.

11. Angular rates in μb/5 degrees of particles exiting 14, 24, and 40 λ_0 of iron.

12. Rates in cm^2/GeV versus k_T for particles exiting a 14 λ_0 absorber for $|\eta| < 3$.

13. The relative fraction of particles exiting a 14 λ_0 absorber with $|\eta| < 3$ versus k_T from (a) prompt decays; (b) π/K decays; and (c) punchthroughs.

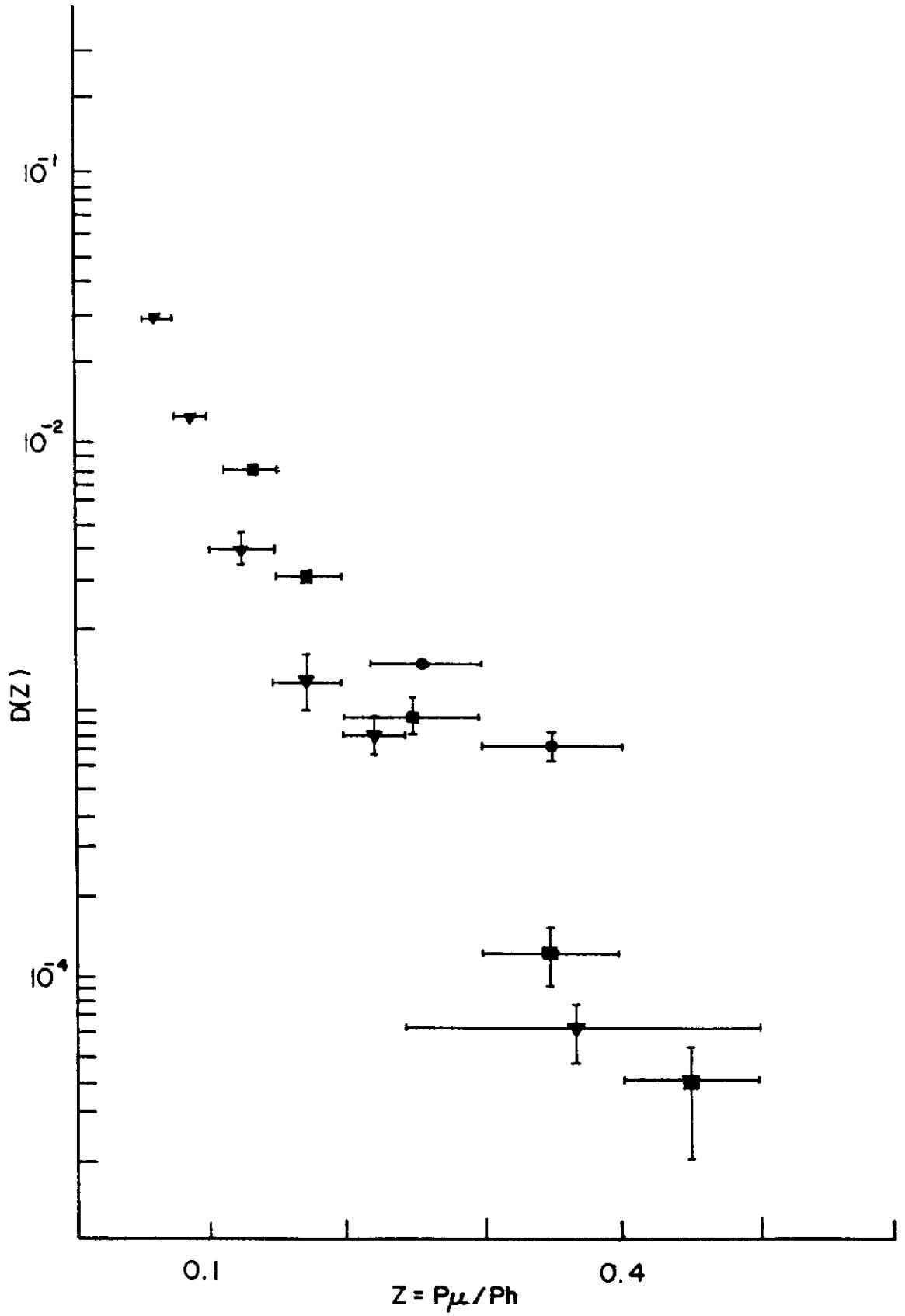

Figure 1

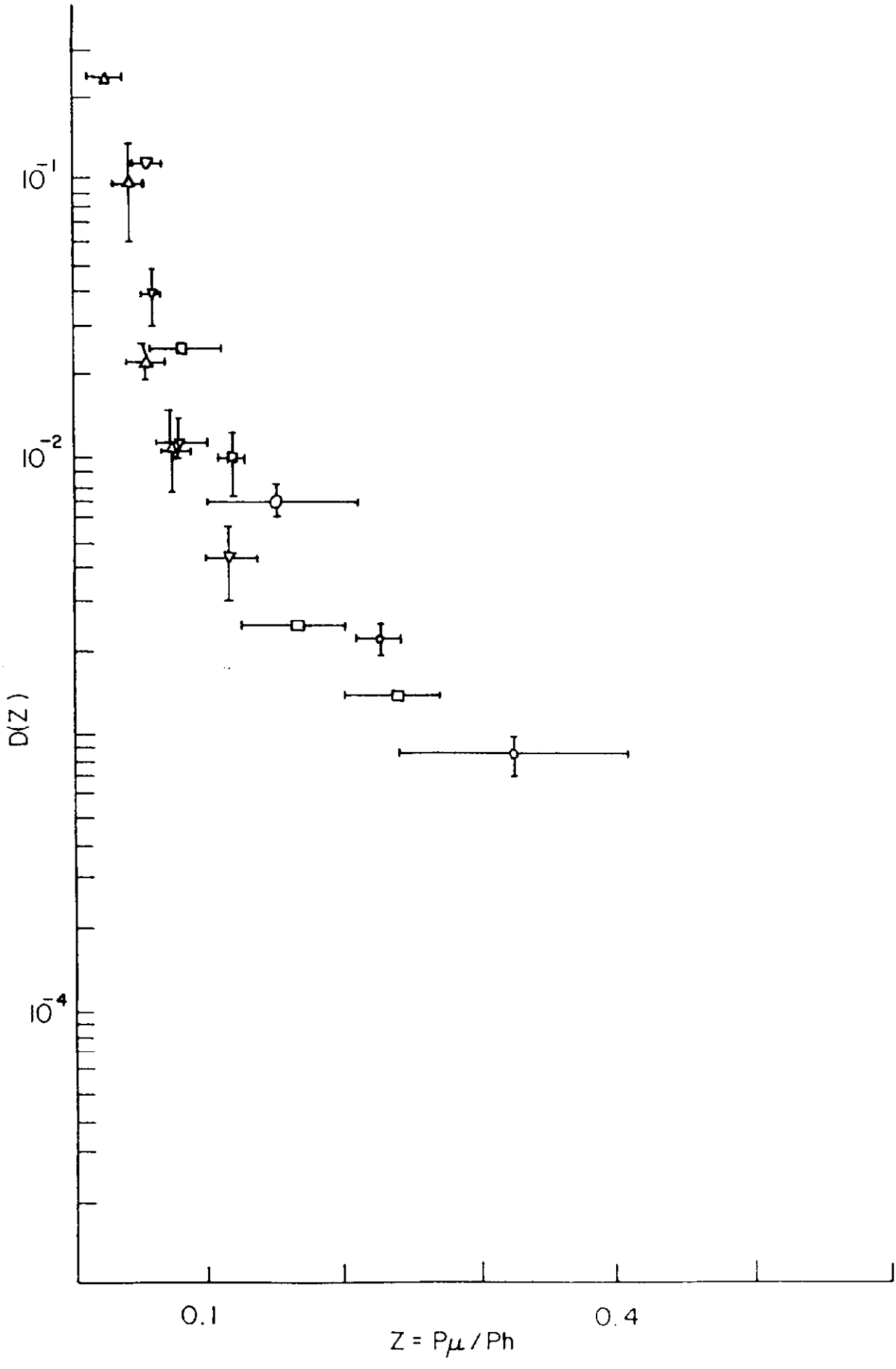

Figure 2

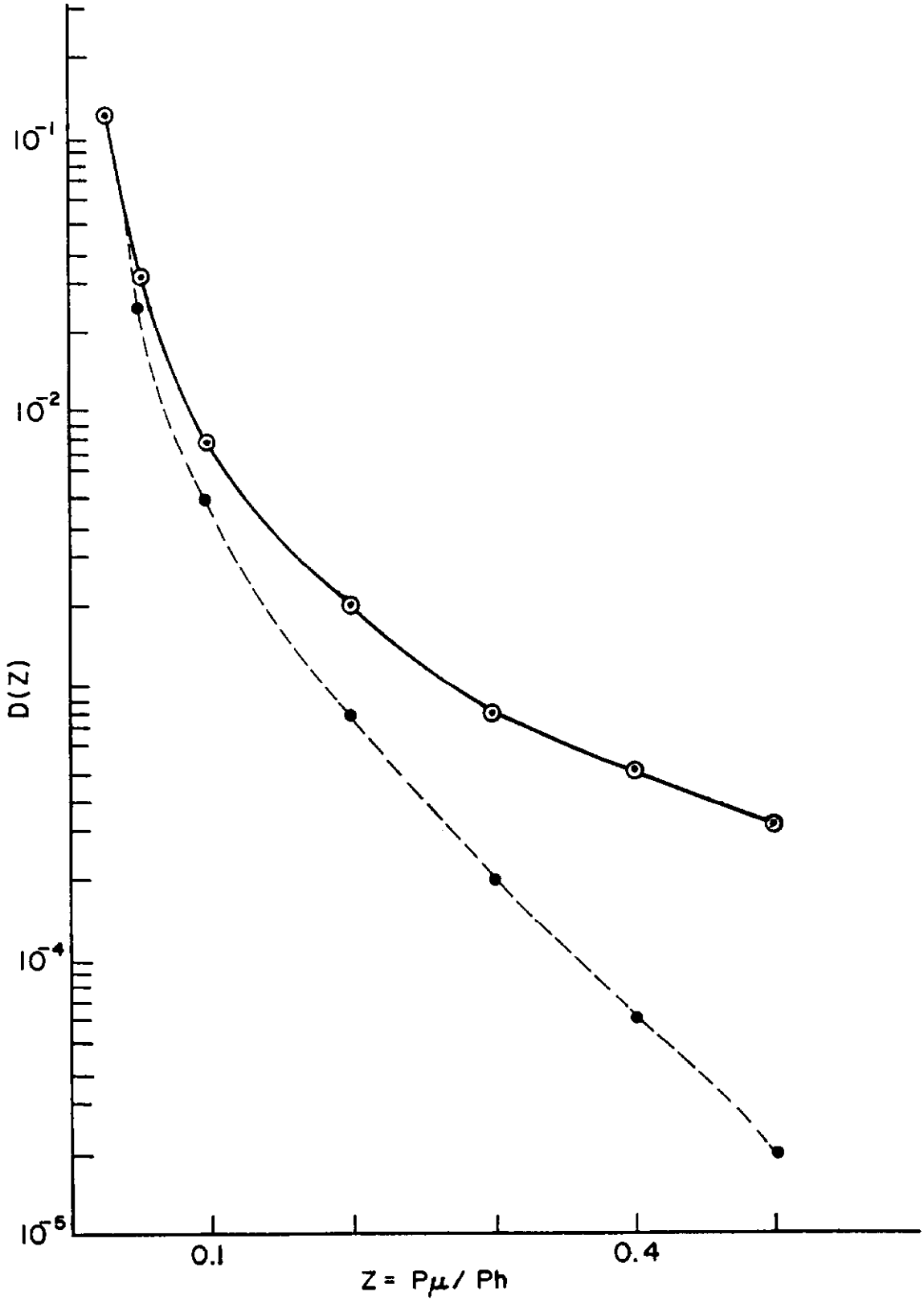

Figure 3

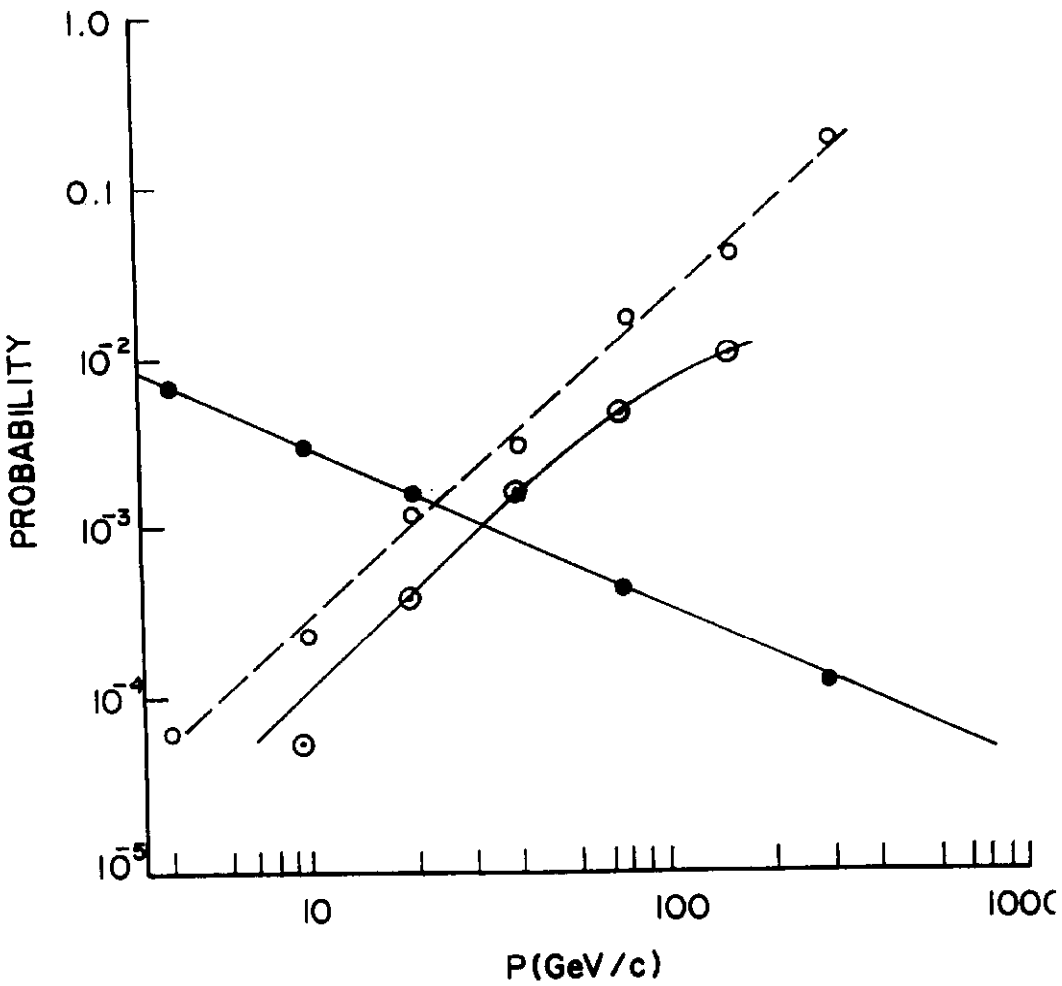

Figure 4

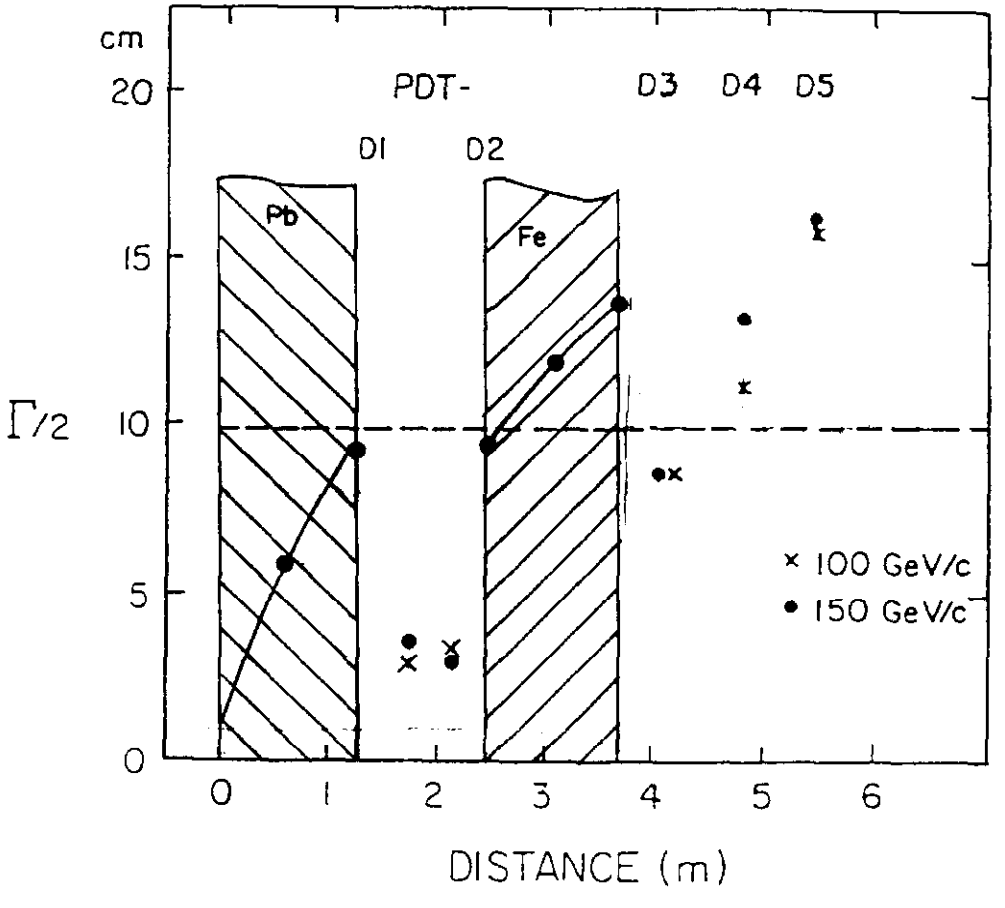
cm
20
15
10
5
0
Γ/2
PDT-
D1
D2
D3
D4
D5
Pb
Fe
× 100 GeV/c
• 150 GeV/c
0
1
2
3
4
5
6
DISTANCE (m)

Figure 5

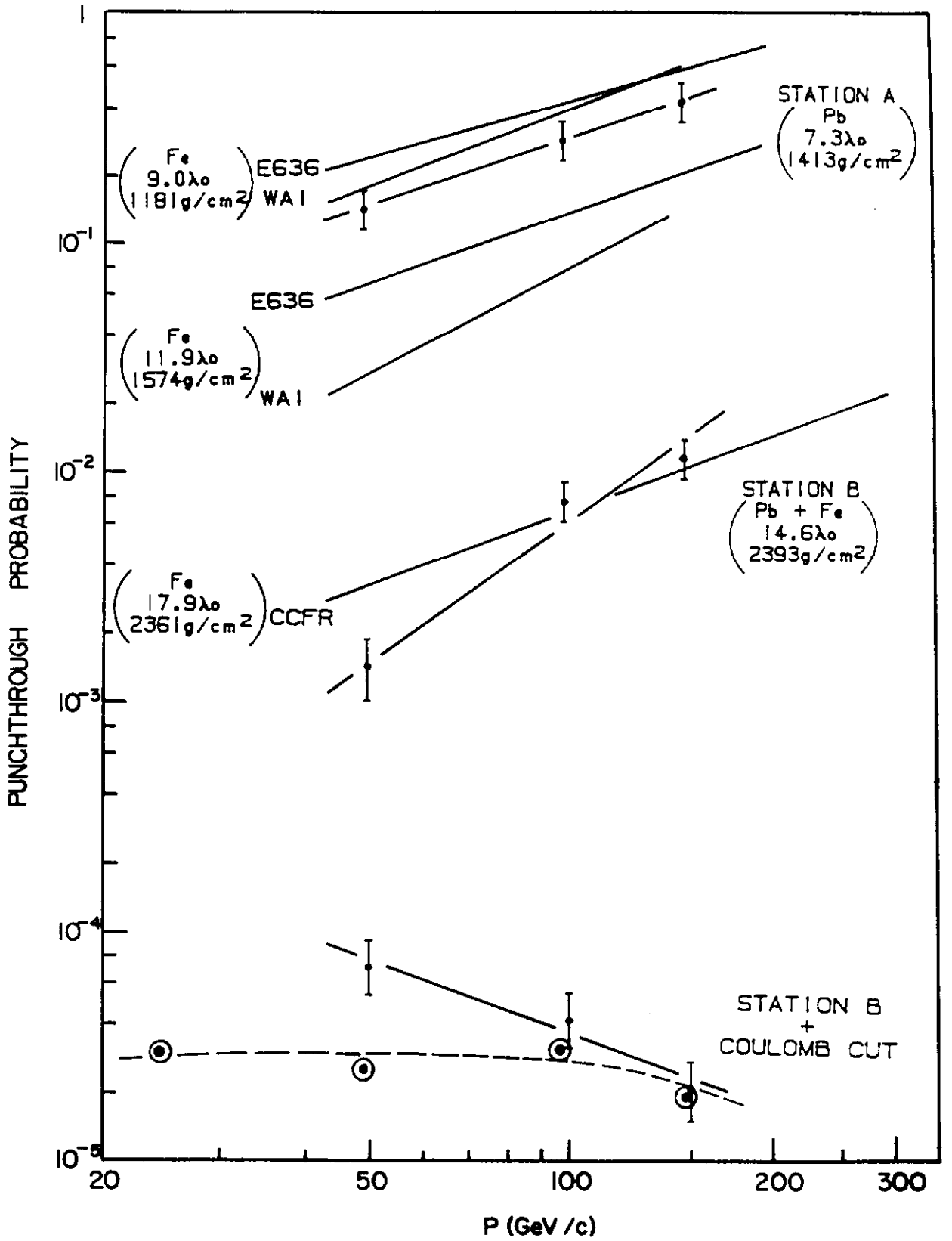
PUNCHTHROUGH PROBABILITY
1
10^{-1}
10^{-2}
10^{-3}
10^{-4}
10^{-5}
20
50
100
200
300
P (GeV/c)
STATION A
Pb
7.3λo
1413g/cm²
E636
WA1
Fe
9.0λo
1181g/cm²
E636
WA1
Fe
11.9λo
1574g/cm²
STATION B
Pb + Fe
14.6λo
2393g/cm²
Fe
17.9λo
2361g/cm²
CCFR
STATION B
+
COULOMB CUT

Figure 6

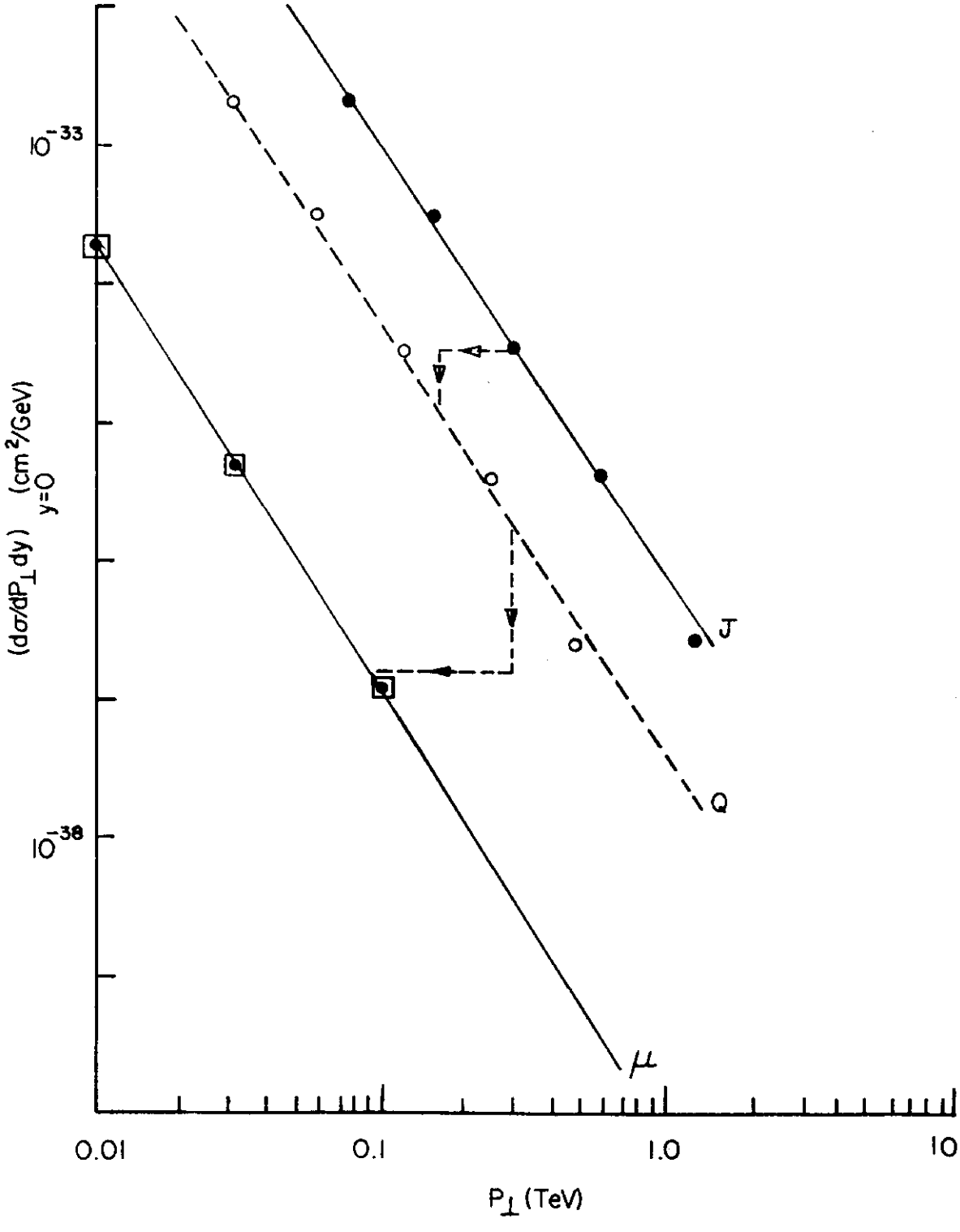
10^{-33}
10^{-38}
$(d\sigma/dP_\perp dy)_{y=0}$ (cm^2/GeV)
J
Q
μ
0.01
0.1
1.0
10
$P_\perp$ (TeV)

Figure 7

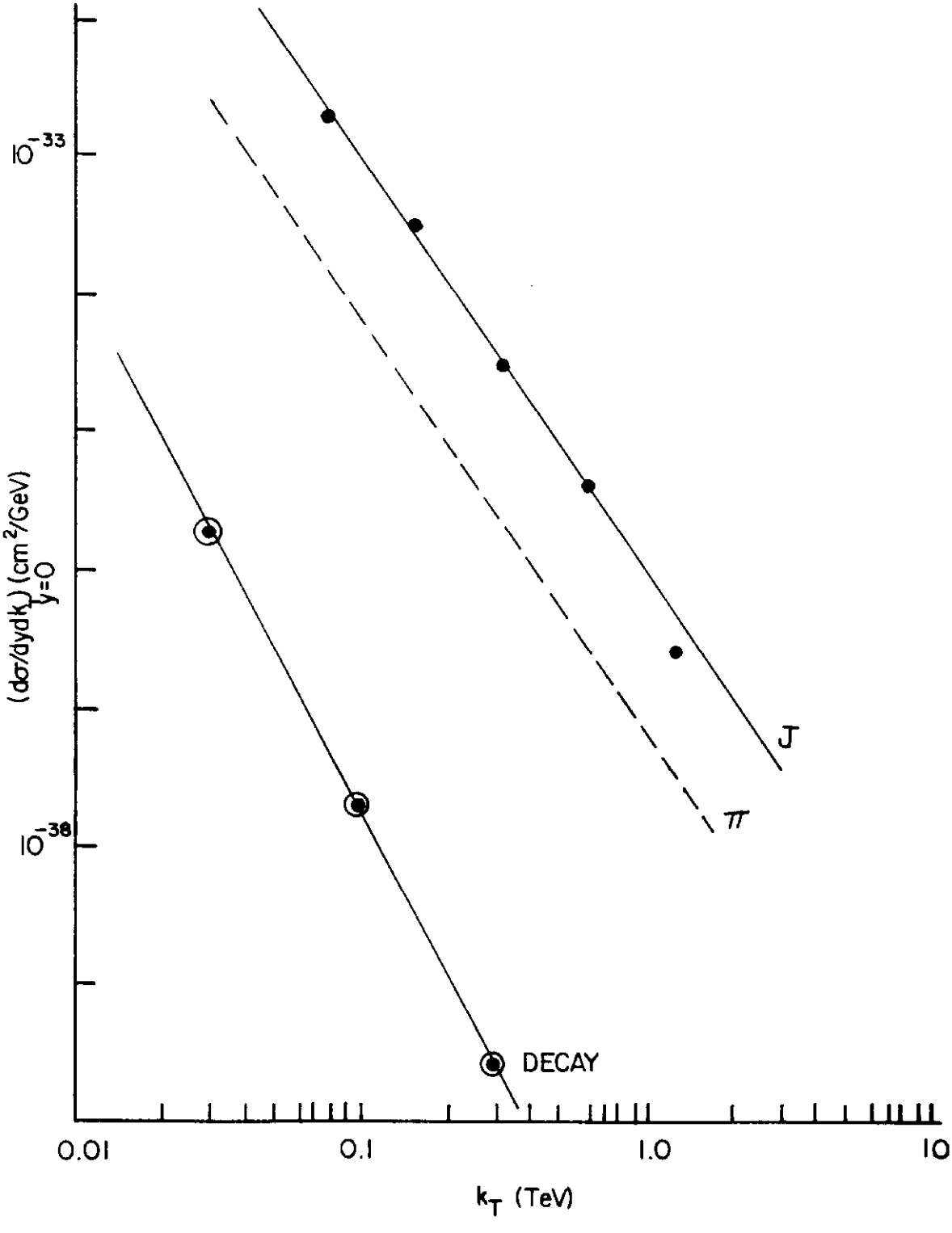

Figure 8

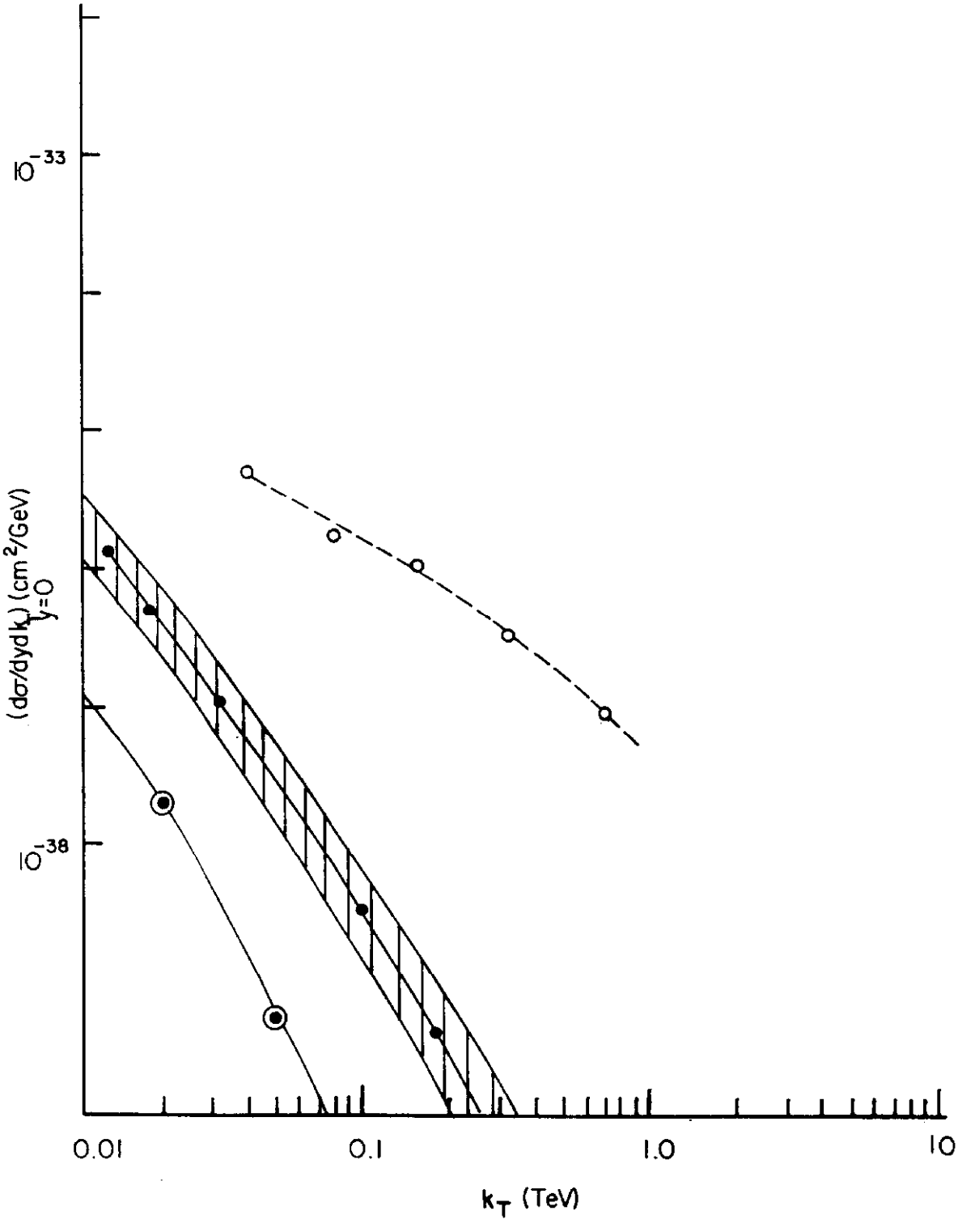

Figure 9

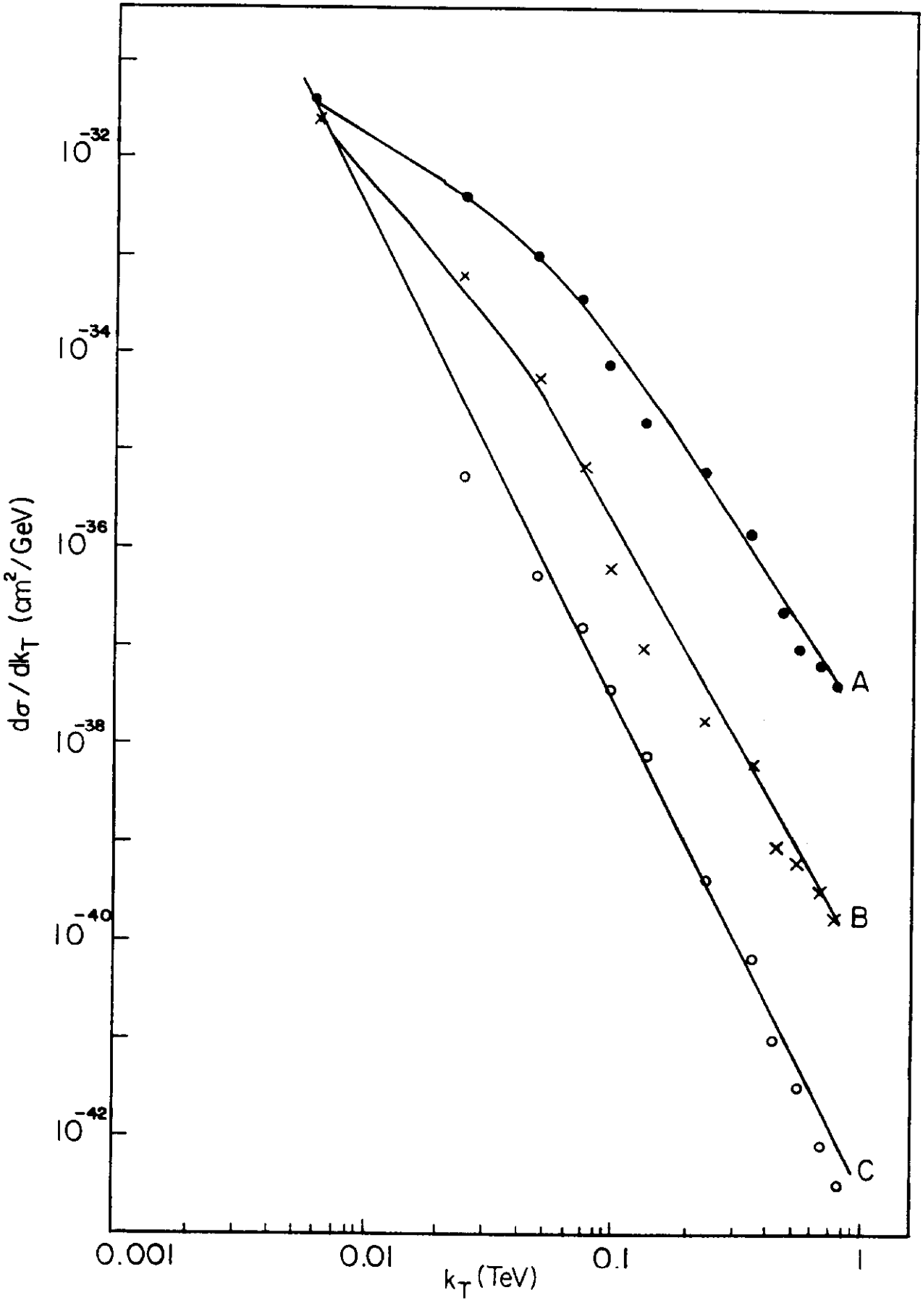
10^{-32}
10^{-34}
10^{-36}
10^{-38}
10^{-40}
10^{-42}
$d\sigma / dk_T$ (cm^2/GeV)
0.001
0.01
0.1
1
k_T (TeV)
A
B
C

Figure 10

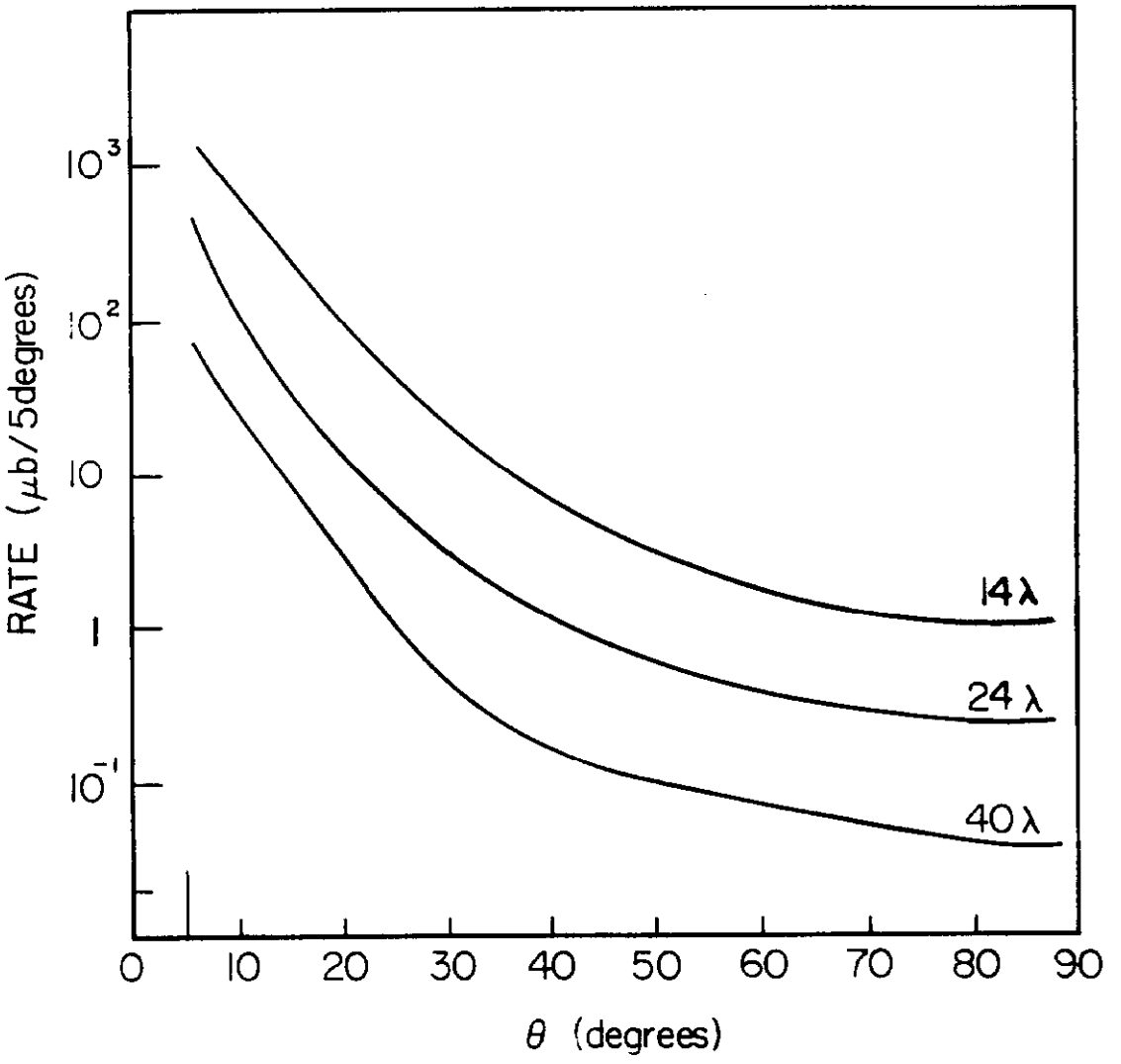
RATE (μb/5degrees)
10³
10²
10
1
10⁻¹
14λ
24λ
40λ
0
10
20
30
40
50
60
70
80
90
θ (degrees)

Figure 11

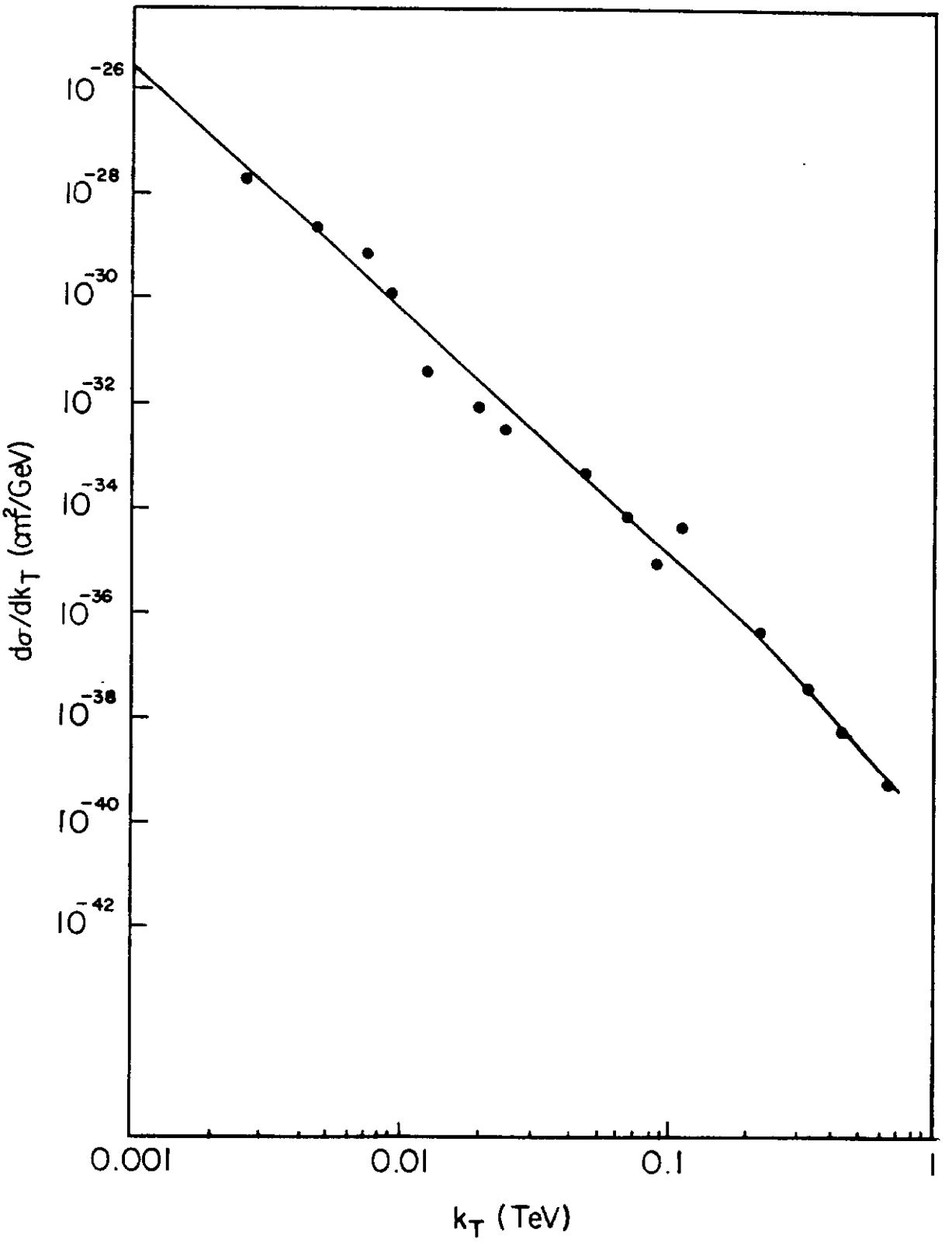
10^{-26}
10^{-28}
10^{-30}
10^{-32}
10^{-34}
10^{-36}
10^{-38}
10^{-40}
10^{-42}
$d\sigma/dk_T$ (cm^2/GeV)
0.001
0.01
0.1
1
k_T (TeV)

Figure 12

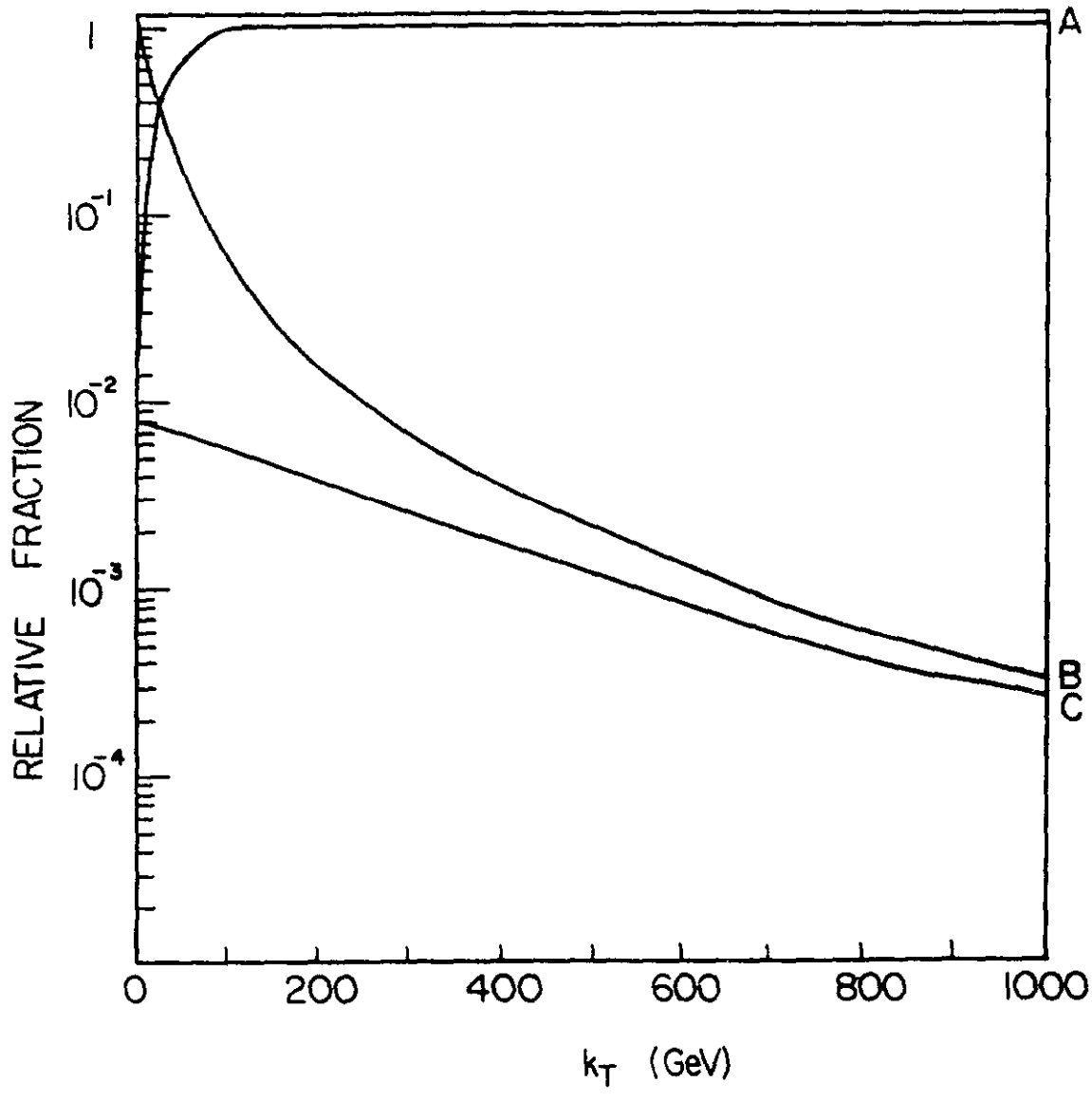
RELATIVE FRACTION
1
10^{-1}
10^{-2}
10^{-3}
10^{-4}
A
B
C
0
200
400
600
800
1000
k_T (GeV)

Figure 13